LETTERS

The scaling laws of human travel

D. Brockmann[1,2], L. Hufnagel[3] & T. Geisel[1,2,4]

The dynamic spatial redistribution of individuals is a key driving force of various spatiotemporal phenomena on geographical scales. It can synchronize populations of interacting species, stabilize them, and diversify gene pools[1–3]. Human travel, for example, is responsible for the geographical spread of human infectious disease[4–9]. In the light of increasing international trade, intensified human mobility and the imminent threat of an influenza A epidemic[10], the knowledge of dynamical and statistical properties of human travel is of fundamental importance. Despite its crucial role, a quantitative assessment of these properties on geographical scales remains elusive, and the assumption that humans disperse diffusively still prevails in models. Here we report on a solid and quantitative assessment of human travelling statistics by analysing the circulation of bank notes in the United States. Using a comprehensive data set of over a million individual displacements, we find that dispersal is anomalous in two ways. First, the distribution of travelling distances decays as a power law, indicating that trajectories of bank notes are reminiscent of scale-free random walks known as Lévy flights. Second, the probability of remaining in a small, spatially confined region for a time T is dominated by algebraically long tails that attenuate the super-diffusive spread. We show that human travelling behaviour can be described mathematically on many spatiotemporal scales by a two-parameter continuous-time random walk model to a surprising accuracy, and conclude that human travel on geographical scales is an ambivalent and effectively superdiffusive process.

Quantitative aspects of dispersal in ecology are based on the dispersal curve, which quantifies the relative frequency of travel distances of individuals as a function of geographical distance[11]. A large class of dispersal curves (for example, exponential, gaussian, stretched exponential) permits the identification of a typical length scale by the variance of the displacement length or equivalent quantities. When interpreted as the probability $P(r)$ of finding a displacement of length r in a short time δt, the existence of a typical length scale often justifies the description of dispersal in terms of diffusion equations on large spatiotemporal scales. If, however, $P(r)$ lacks a typical length scale, that is $P(r) \sim r^{-(1+\beta)}$ with $\beta < 2$, the diffusion approximation fails. In physics, random processes with such a single-step distribution are known as Lévy flights[12–16] (see Supplementary Information). Recently, the related notion of long-distance-dispersal (LDD) has been established in dispersal ecology[17], taking into account the observation that dispersal curves of a number of species show power-law tails owing to long-range movements[18–21]. (In ecological literature, the term 'dispersal' is commonly used in the context of the spatial displacement of individuals of a species between their geographical origin of birth and the location of their first breeding place. Here we use the term dispersal to refer to geographical displacements that occur on much shorter timescales, that is, due to travel by various means of transportation.)

Nowadays, humans travel on many spatial scales, ranging from a few to thousands of kilometres over short periods of time. The direct quantitative assessment of human movements, however, is difficult, and a statistically reliable estimate of human dispersal comprising all spatial scales does not exist. The central aim of this work is to use data collected at online bill-tracking websites (which monitor the world-wide dispersal of large numbers of individual bank notes) to infer the statistical properties of human dispersal with very high spatio-temporal precision. Our analysis of human movement is based on the trajectories of 464,670 dollar bills obtained from the bill-tracking system www.wheresgeorge.com. We analysed the dispersal of bank notes in the United States, excluding Alaska and Hawaii. The core data consists of 1,033,095 reports to the bill-tracking website. From these reports we calculated the geographical displacements $r = |\mathbf{x}_2 - \mathbf{x}_1|$ between a first ($\mathbf{x}_1$) and secondary ($\mathbf{x}_2$) report location of a bank note and the elapsed time T between successive reports.

In order to illustrate qualitative features of bank note trajectories, Fig. 1b depicts short-time trajectories ($T < 14$ days) originating from three major US cities: Seattle, New York and Jacksonville. After their initial entry into the tracking system, most bank notes are next reported in the vicinity of the initial entry location, that is $|\mathbf{x}_2 - \mathbf{x}_1| \leq 10$ km (Seattle, 52.7%; New York, 57.7%; Jacksonville, 71.4%). However, a small but considerable fraction is reported beyond a distance of 800 km (Seattle, 7.8%; New York, 7.4%; Jacksonville, 2.9%).

From a total of 20,540 short-time trajectories originating across the United States, we measured the probability $P(r)$ of traversing a distance r in a time interval δT of 1–4 days (Fig. 1c). A total of 14,730 (that is, a fraction $Q = 0.71$) secondary reports occurred outside a short range radius $L_{\min} = 10$ km. Between $L_{\min}$ and the approximate average East–West extension of the United States, $L_{\max} \approx 3{,}200$ km, the kernel shows power-law behaviour $P(r) \sim r^{-(1+\beta)}$ with an exponent $\beta = 0.59 \pm 0.02$. For $r < L_{\min}$, $P(r)$ increases linearly with r, which implies that displacements are distributed uniformly inside the disk $|\mathbf{x}_2 - \mathbf{x}_1| \leq L_{\min}$. We measured $P(r)$ for three classes of initial entry locations: highly populated metropolitan areas (191 sites, local population $N_{\text{loc}} > 120{,}000$), cities of intermediate size (1,544 sites, local population $120{,}000 > N_{\text{loc}} > 22{,}000$) and small towns (23,640 sites, local population $N_{\text{loc}} < 22{,}000$), comprising 35.7%, 29.1% and 25.2% of the entire population of the United States, respectively. The inset in Fig. 1c shows $P(r)$ for these classes. Despite systematic deviations for short distances, all distributions show an algebraic tail with the same exponent $\beta \approx 0.6$, which confirms that the observed power-law is an intrinsic and universal property of dispersal.

However, the situation is more complex. If we assume that the dispersal of bank notes can be described by a Lévy flight with a short-time probability distribution $P(r)$, we can estimate the time T_{eq} for an initially localized ensemble of bank notes to reach the stationary distribution[22] (maps in Fig. 1a), obtaining a value of $T_{\text{eq}} \approx 68$ days (see Supplementary Information). Thus, after 2–3 months, bank notes should have reached an equilibrium distribution. Surprisingly, the long-time dispersal data does not reflect a relaxation within this

[1]Max-Planck Institute for Dynamics and Self-Organisation, Bunsenstr. 10, 37073 Göttingen, Germany. [2]Department of Physics, University of Göttingen, 37073 Göttingen, Germany. [3]Kavli Institute for Theoretical Physics, University of California, Santa Barbara, California 93106, USA. [4]Bernstein Center for Computational Neuroscience, 37073 Göttingen, Germany.

time. Figure 1b shows secondary reports of bank notes with initial entry at Omaha that have dispersed for times $T > 100$ days (with an average time $\langle T \rangle = 289$ days). Only 23.6% of the bank notes travelled farther than 800 km, whereas 57.3% travelled an intermediate distance $50 < r < 800$ km, and a relatively large fraction of 19.1% remained within a radius of 50 km, even after an average time of nearly one year. From the computed value $T_{eq} \approx 68$ days, a much higher fraction of bills is expected to reach the metropolitan areas of the West coast and the New England states after this time. This is sufficient evidence that the simple Lévy flight picture for dispersal is incomplete. What causes this attenuation of dispersal?

Two alternative explanations might account for this effect. The slowing down might be caused by strong spatial inhomogeneities of the system. People might be less likely to leave large cities than for example, suburban areas. Alternatively, long periods of rest might be an intrinsic temporal property of dispersal. In as much as an algebraic tail in spatial displacements yields superdiffusive behaviour, a tail in the probability density $\phi(t)$ for times t between successive spatial displacements of an ordinary random walk can lead to subdiffusion[15] (see Supplementary Information). Here, the ambivalence between scale-free spatial displacements and scale-free periods of rest can be responsible for the observed attenuation of superdiffusion.

In order to address this issue we investigated the relative proportion $P_0^i(t)$ of bank notes which are reported in a small (20 km) radius of the initial entry location i as a function of time (Fig. 1d). The quantity $P_0^i(t)$ estimates the probability of a bank note being reported at the initial location at time t. We computed $P_0^i(t)$ for metropolitan areas, cities of intermediate size and small towns: for all classes we found the asymptotic behaviour $P_0(t) \sim At^{-\eta}$, with the same exponent $\eta = 0.6 \pm 0.03$, which indicates that waiting time and dispersal characteristics are universal. Notice that for a pure Lévy flight with index β in two dimensions, $P_0(t)$ scales with time as $t^{-2/\beta}$ (dashed red line)[15]. For $\beta \approx 0.6$ (as suggested by Fig. 1c) this implies $\eta \approx 3.33$. This is a fivefold steeper decrease than observed, which clearly shows that dispersal cannot be described by a pure Lévy flight. The measured decay is even slower than the decay expected from ordinary two-dimensional diffusion ($\eta = 1$, dashed black line). Therefore, we conclude that the slow decay in $P_0(t)$ reflects the effect

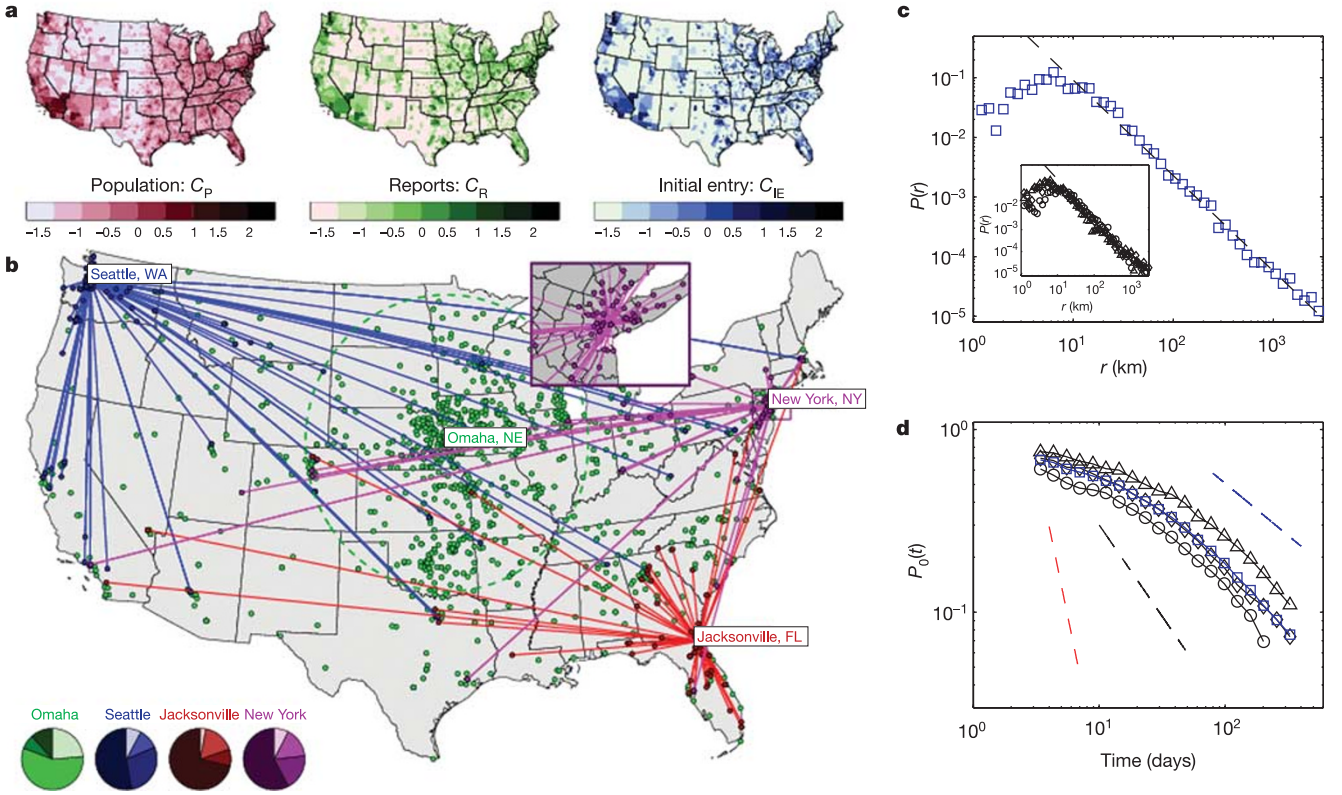

Figure 1 | Dispersal of bank notes and humans on geographical scales. **a**, Relative logarithmic densities of population ($c_P = \log \rho_P / \langle \rho_P \rangle$), report ($c_R = \log \rho_R / \langle \rho_R \rangle$) and initial entry ($c_{IE} = \log \rho_{IE} / \langle \rho_{IE} \rangle$) as functions of geographical coordinates. Colour-code shows densities relative to the nationwide averages (3,109 counties) of $\langle \rho_P \rangle = 95.15$, $\langle \rho_R \rangle = 0.34$ and $\langle \rho_{IE} \rangle = 0.15$ individuals, reports and initial entries per km^2, respectively. **b**, Trajectories of bank notes originating from four different places. City names indicate initial location, symbols secondary report locations. Lines represent short-time trajectories with travelling time $T < 14$ days. Lines are omitted for the long-time trajectories (initial entry in Omaha) with $T > 100$ days. The inset depicts a close-up view of the New York area. Pie charts indicate the relative number of secondary reports coarsely sorted by distance. The fractions of secondary reports that occurred at the initial entry location (dark), at short ($0 < r < 50$ km), intermediate ($50 < r < 800$ km) and long ($r > 800$ km) distances are ordered by increasing brightness of hue. The total number of initial entries are $N = 2{,}055$ (Omaha), $N = 524$ (Seattle), $N = 231$ (New York), $N = 381$ (Jacksonville). **c**, The short-time dispersal kernel. The measured probability density function $P(r)$ of traversing a distance r in less than $T = 4$ days is depicted in blue symbols. It is computed from an ensemble of 20,540 short-time displacements. The dashed black line indicates a power law $P(r) \sim r^{-(1+\beta)}$ with an exponent of $\beta = 0.59$. The inset shows $P(r)$ for three classes of initial entry locations (black triangles for metropolitan areas, diamonds for cities of intermediate size, circles for small towns). Their decay is consistent with the measured exponent $\beta = 0.59$ (dashed line). **d**, The relative proportion $P_0(t)$ of secondary reports within a short radius ($r_0 = 20$ km) of the initial entry location as a function of time. Blue squares show $P_0(t)$ averaged over 25,375 initial entry locations. Black triangles, diamonds, and circles show $P_0(t)$ for the same classes as **c**. All curves decrease asymptotically as $t^{-\eta}$ with an exponent $\eta = 0.60 \pm 0.03$ indicated by the blue dashed line. Ordinary diffusion in two dimensions predicts an exponent $\eta = 1.0$ (black dashed line). Lévy flight dispersal with an exponent $\beta = 0.6$ as suggested by **b** predicts an even steeper decrease, $\eta = 3.33$ (red dashed line).

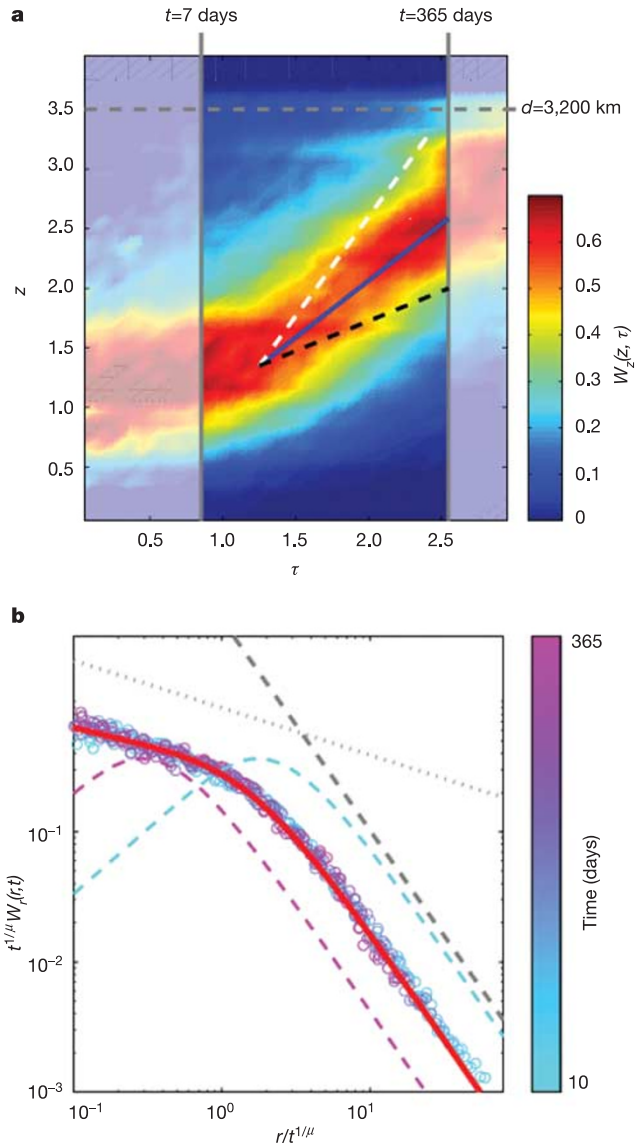

Figure 2 | Spatiotemporal scaling of bank note dispersal. **a**, The probability density $W_z(z,\tau)$ of having travelled a logarithmic distance $z = \log_{10} r$ at logarithmic time $\tau = \log_{10} t$. The middle segment indicates the scaling regime between one week and one year. The superimposed red line represents the scaling behaviour $r(t) \sim t^{1/\mu}$ with exponent $\mu = 1.05 \pm 0.05$. It is compared to the diffusive scaling (black dashed line) and the scaling of a pure Lévy process with exponent $\beta = 0.6$ (white dashed line). The upper dashed grey line shows the approximate linear extent $L_{\max} = 3{,}200$ km of the United States. **b**, The measured radial probability density $W_r(r,t)$ and theoretical scaling function $L_{\alpha,\beta}(r/t^{1/\mu})$ (equation (2)). In order to extract the quality of scaling, the function $t^{1/\mu}W_r(r,t)$ is shown for various but fixed values of t from 10–365 days as a function of the rescaled distance $r/t^{1/\mu}$, where the exponent μ was set to the value determined in **a**. As the measured (circles) curves collapse on a single curve, the process shows universal scaling. The scaling curve represents the limiting density of the process. The asymptotic behaviour for small (grey dotted line) and large (grey dashed line) arguments $y = r/t^{1/\mu}$ is given by $y^{-(1-\xi_1)}$ and $y^{-(1+\xi_2)}$, respectively, with estimated exponents $\xi_1 = 0.63 \pm 0.04$ and $\xi_2 = 0.62 \pm 0.02$. According to our model, these exponents must fulfill $\xi_1 = \xi_2 = \beta$, where β is the exponent of the asymptotic short-time dispersal kernel (Fig. 1c), that is $\beta \approx 0.6$. The superimposed red line represents $t^{1/\mu}W_r(r,t)$ predicted by our theory, with spatial and temporal exponents $\alpha = 0.6$ and $\beta = 0.6$, respectively. The coloured dashed lines represent $t^{1/\mu}W_r(r,t)$ for a pure Lévy flight with $\beta = 0.6$ at times $t = 10$ and $t = 365$ days. The curves do not collapse because the pure Lévy flight shows the wrong spatiotemporal scaling. Furthermore, the limiting curves strongly deviate from the data for small arguments.

of an algebraic tail in the distribution of rests $\phi(t)$ between displacements. Indeed, if $\phi(t) \sim t^{-(1+\alpha)}$ with $\alpha < 1$, then $\eta = \alpha$ and consequently $\alpha = 0.60 \pm 0.03$. This suggests that an algebraic tail in the distribution of rests $\phi(t)$ is responsible for slowing down the superdiffusive dispersal advanced by the short time dispersal kernel in Fig. 1c.

In order to model the antagonistic interplay between scale-free displacements and waiting times, we use the framework of continuous-time random walks (CTRW) introduced by Montroll and Weiss[23]. A CTRW consists of a succession of random displacements $\delta\mathbf{x}_n$ and random waiting times δt_n, each of which is drawn from a corresponding probability density function $P(\delta\mathbf{x}_n)$ and $\phi(\delta t)$. After N iterations, the position of the walker and the elapsed time are given by $\mathbf{x}_N = \sum_n \delta\mathbf{x}_n$ and $t_N = \sum_n \delta t_n$. The quantity of interest is the position $\mathbf{x}(t)$ after time t and the associated probability density $W(\mathbf{x},t)$ that can be computed within CTRW theory. For displacements with finite variance σ^2 and waiting times with finite mean τ, such a CTRW yields ordinary diffusion asymptotically, that is $\partial_t W(\mathbf{x},t) = D\partial_x^2 W(\mathbf{x},t)$ with a diffusion coefficient $D = \sigma^2/\tau$.

In contrast, we assume here that both $P(\delta\mathbf{x}_n)$ and $\phi(\delta t)$ show algebraic tails, that is $P(\delta\mathbf{x}_n) \sim |\delta\mathbf{x}_n|^{-(1+\beta)}$ and $\phi(\delta t) \sim |\delta t|^{-(1+\alpha)}$, for which σ^2 and τ are infinite. In this case we can derive a bifractional diffusion equation for the dynamics of $W(\mathbf{x},t)$:

$$\partial_t^{\alpha} W(\mathbf{x},t) = D_{\alpha,\beta}\partial_{|x|}^{\beta} W(\mathbf{x},t) \qquad (1)$$

In this equation, the symbols ∂_t^{α} and $\partial_{|x|}^{\beta}$ denote fractional derivatives that are non-local and depend on the tail exponents α and β. The constant $D_{\alpha,\beta}$ is a generalized diffusion coefficient (see Supplementary Information). Equation (1) represents the core dynamical equation of our model. Using methods of fractional calculus we can solve this equation and obtain the probability $W_r(r,t)$ of having traversed a distance r at time t:

$$W_r(r,t) = t^{-\alpha/\beta} L_{\alpha,\beta}(r/t^{\alpha/\beta}) \qquad (2)$$

where $L_{\alpha,\beta}$ is a universal scaling function that represents the characteristics of the process. Equation (2) implies that the typical distance travelled scales according to $r(t) \sim t^{1/\mu}$, where $\mu = \beta/\alpha$. Thus, depending on the ratio of spatial and temporal exponents, the random walk can be effectively either superdiffusive ($\beta < 2\alpha$), subdiffusive ($\beta > 2\alpha$), or quasidiffusive ($\beta = 2\alpha$) (see Supplementary Information). For the exponents observed in the dispersal data ($\beta = 0.59 \pm 0.02$ and $\alpha = 0.60 \pm 0.03$) the theory predicts a temporal scaling exponent in the vicinity of unity, $\mu = 0.98 \pm 0.08$. Therefore, dispersal remains superdiffusive despite long periods of rest.

The validity of our model can be tested by estimating $W_r(r,t)$ from the entire data set of a little over half a million displacements and elapse times. The scaling property is best extracted from the data by a transformation to logarithmic coordinates $z = \log_{10} r$, $\tau = \log_{10} t$ and the associated probability density $W_z(z,\tau)$. If the original process scales according to $r(t) \sim t^{1/\mu}$, the density $W_z(z,\tau)$ is a function of $z - \tau/\mu$ only. Figure 2a shows that scaling occurs in a time window of approximately seven days to one year. From the slope (blue line), we obtain a scaling exponent $\mu = 1.05 \pm 0.02$, which agrees well with our model.

Finally, we investigated the degree to which bank note dispersal shows a scaling density as predicted by our model (that is, the relation outlined in equation(2)). Figure 2b shows $t^{1/\mu}W_r(r,t)$ extracted from data versus the ratio $y = r/t^{1/\mu}$. The exponent $\mu = 1.05$ was set to the value obtained in Fig. 2a. The collapse of the data on a single curve indicates that in the chosen time interval of 10–365 days, bank note dispersal shows a universal scaling function. The asymptotic behaviour of the empirical curve is given by $y^{-(1-\xi_1)}$ and $y^{-(1+\xi_2)}$ for small and large arguments, respectively. Both exponents fulfil $\xi_1 \approx \xi_2 \approx 0.6$. We compared the empirical curve with the theoretical prediction of our model. By series expansions, we can compute the asymptotics of the limiting function $L_{\alpha,\beta}(y)$ in equation (2),

giving $y^{-(1-\beta)}$ and $y^{-(1+\beta)}$ for small and large y, respectively. Consequently, as $\beta \approx 0.6$ (Fig. 1c), the theory agrees well will the observed exponents. For the entire range of y we computed $L_{\alpha,\beta}(y)$ by numeric integration for $\alpha = \beta = 0.6$, and superimposed the theoretical curve on the empirical one. The agreement is very satisfactory. In summary, our analysis gives solid evidence that the dispersal of bank notes can be accounted for by our model.

The question remains how the dispersal characteristics of bank notes carry over to the travelling behaviour of humans. In this context, we can conclude that the power law with exponent $\beta = 0.6$ of the short-time dispersal kernel for bank notes reflects the human dispersal kernel, because the exponent remains unchanged for short time intervals of $T = 2$, 4, 7 and 14 days. The issue of long waiting times is more subtle. One might speculate that the observed algebraic tail in waiting times of bank notes is a property of bank note dispersal alone. Long waiting times might be caused by bank notes that exit the money-tracking system for a long time, for instance in banks. However, if this were the case the inter-report time statistics would have an algebraic tail as well. Analysing the inter-report time distribution, we found an exponential decay, suggesting that bank notes are passed from person to person at a constant rate. If we assume that humans exit small areas at a constant rate that is equivalent to exponentially distributed waiting times, and that bank notes pass from person to person at a constant rate, the distribution of bank note waiting times would also be exponential, in contrast to the observed power law. To our minds, this reasoning permits no other conclusion than a lack of scale in human waiting-time statistics. We obtained further support for our results from a comparison with two independent human travel data sets: long-distance travel on the United States aviation network[8] (flight schedules and airport information, www.oag.com; International Air Transport Association, www.iata.org) and the latest survey on long-distance travel conducted by the United States Bureau of Transportation Statistics (www.bts.gov) (see Supplementary Information). Both agree well with our findings and support our conclusions.

On the basis of our analysis, we conclude that the dispersal of bank notes and human travel behaviour can be described by a continuous-time random-walk process that incorporates scale-free jumps as well as long waiting times between displacements. To our knowledge, this is the first empirical evidence for such an ambivalent process in nature. We believe that these results can serve as a starting point for the development of a new class of models for the spread of human infectious diseases, because universal features of human travel can now be accounted for in a quantitative way.

Received 13 July; accepted 3 October 2005.

1. Bullock, J. M., Kenward, R. E. & Hails, R. S. (eds) *Dispersal Ecology* (Blackwell, Malden, Massachusetts, 2002).
2. Murray, J. D. *Mathematical Biology* (Springer-Verlag, New York, 1993).
3. Clobert, J., Danchin, E., Dhondt, A. A. & Nichols, J. D. (eds) *Dispersal* (Oxford Univ. Press, Oxford, 2001).
4. Nicholson, K. & Webster, R. G. *Textbook of Influenza* (Blackwell, Malden, Massachusetts, 1998).
5. Grenfell, B. T., Bjornstadt, O. N. & Kappey, J. Travelling waves and spatial hierarchies in measles epidemics. *Nature* **414,** 716–723 (2001).
6. Keeling, M. J. *et al.* Dynamics of the 2001 UK foot and mouth epidemic: stochastic dispersal in a heterogeneous landscape. *Science* **294,** 813–817 (2001).
7. Hudson, P. J., Rizzoli, A., Grenfell, B. T. & Heesterbeek, H. (eds) *The Ecology of Wildlife Diseases* (Oxford Univ. Press, Oxford, 2002).
8. Hufnagel, L., Brockmann, D. & Geisel, T. Forecast and control of epidemics in a globalized world. *Proc. Natl Acad. Sci. USA* **101,** 15124–15129 (2004).
9. Grassly, N. C., Fraser, C. & Garnett, G. P. Host immunity and synchronized epidemics of syphilis across the United States. *Nature* **433,** 417–421 (2005).
10. Webby, R. J. & Webster, R. G. Are we ready for pandemic influenza? *Science* **302,** 1519–1522 (2003).
11. Kot, M., Lewis, M. A. & van den Driessche, P. Dispersal data and the spread of invading organisms. *Ecology* **77,** 2027–2042 (1996).
12. Shlesinger, M. F., Zaslavsky, G. M. & Frisch, U. (eds) *Lévy Flights and Related Topics in Physics* (Springer Verlag, Berlin, 1995).
13. Klafter, J., Shlesinger, M. F. & Zumofen, G. Beyond Brownian motion. *Phys. Today* **49,** 33–39 (1996).
14. Brockmann, D. & Geisel, T. Lévy flights in inhomogeneous media. *Phys. Rev. Lett.* **90,** 170601 (2003).
15. Metzler, R. & Klafter, J. The random walks guide to anomalous diffusion: a fractional dynamics approach. *Phys. Rep.* **339,** 1–77 (2000).
16. Shlesinger, M. F., Klafter, J. & Wong, Y. M. Random-walks with infinite spatial and temporal moments. *J. Stat. Phys.* **27,** 499–512 (1982).
17. Nathan, R. The challenges of studying dispersal. *Trends Ecol. Evol.* **16,** 481–483 (2001).
18. Viswanathan, G. M. *et al.* Lévy flight search patterns of wandering albatrosses. *Nature* **381,** 413–415 (1996).
19. Ramos-Fernandéz, G., Mateos, J. L., Miramontes, O. & Cocho, G. Lévy walk patterns in the foraging movements of spider monkeys. *Behav. Ecol. Sociobiol.* **55,** 223–230 (2004).
20. Levin, S. A., Muller-Landau, H. C., Nathan, R. & Chave, J. The ecology and evolution of seed dispersal: A theoretical perspective. *Annu. Rev. Ecol. Evol. Syst.* **34,** 575–604 (2003).
21. Nathan, R. *et al.* Mechanisms of long-distance dispersal of seeds by wind. *Nature* **418,** 409–413 (2002).
22. Gardiner, C. W. *Handbook of Stochastic Methods* (Springer Verlag, Berlin, 1985).
23. Montroll, E. W. & Weiss, G. H. Random walks on lattices. *J. Math. Phys.* **6,** 167–181 (1965).

Supplementary Information is linked to the online version of the paper at www.nature.com/nature.

Acknowledgements We would like to thank the initiators of the bill tracking system (www.wheresgeorge.com). We thank cabinetmaker D. Derryberry for discussions and for drawing our attention to the wheresgeorge website, and B. Shraiman, D. Cohen and W. Noyes for critical comments on the manuscript.

Author Contributions The project idea was conceived by D.B. and L.H., data pre-processing was done by L.H., data analysis by D.B. and L.H., the theory and model was constructed by D.B., and the manuscript was written by D.B., L.H. and T.G.

Author Information Reprints and permissions information is available at npg.nature.com/reprintsandpermissions. The authors declare no competing financial interests. Correspondence and requests for materials should be addressed to D.B. (brockmann@ds.mpg.de).